



Numerical simulation of cavitating flow past cylinders

Warn-Gyu Park*, Tae-Kyoung Koo*, Chul-Min Jung** and Kurnchul Lee**

* School of Mechanical Engineering, Pusan National University, Pusan, Korea
(Tel : +82-51-510-2457; E-mail: wgpark@pusan.ac.kr)

**Agency for Defense Development, P.O. Box 18, Jinhae, Kyungnam, Korea

Abstract: The cavitating flow simulation is of practical importance for many engineering systems, such as marine propellers, pump impellers, nozzles, injectors, torpedoes, etc. The present work has developed a base code for simulating cavitating flows past cylinders and hydrofoils. The governing equation is the Navier-Stokes equation based on homogeneous mixture model. The momentum and energy equation is in the mixture phase while the continuity equation is solved in liquid and vapor phase, separately. The solver employs an implicit preconditioning algorithm in curvilinear coordinates. The computations have been carried out for the cylinders with spherical, 1- and 0-caliber forebody and hydrofoil of ALE and NACA cross-section and, then, compared with experiments and other numerical results. Fairly good agreements with experiments and numerical results have been achieved. The present base code has shown the feasibility to solve the cavitating flow past supercavitating torpedo after the improvement for compressibility effects and interactions with hot exhaust gas of propulsive rocket.

Keywords: cavitating flow, RANS equations, homogeneous mixture model, preconditioning technique

1. INTRODUCTION

Cavitation generally occurs if the pressure in a certain region of liquid flow drops below the vapor pressure and, consequently, the liquid is vaporized and filled with cavity. The cavitating flow is observed in various propulsion systems and high-speed underwater objects, such as marine propellers, impellers of turbo-machinery, hydrofoils, nozzles, injectors and torpedoes. This phenomenon usually causes severe noise, vibration and erosion.

Even though cavitating flow is a complex phenomenon which has not been completely modeled, a lot of attention was gathered in CFD community as the methodologies for single-phase flow was relatively much matured.

In solving multiphase flows by CFD method, there can be categorized into three groups: The first group uses a single continuity equation [1,2]. This method has been known that it is unable to distinguish between condensable and non-condensable gas [3]. Next group is to solve separate continuity equations for liquid and vapor phase by adding source terms of mass transfer between phase-changes [3-7]. This model is usually so called 'homogeneous mixture model' because the liquid-gas interface is assumed to be in dynamically and thermally equilibrium and, consequently, mixture momentum and energy equations are used. Final group solves full two-fluid modeling, wherein separate momentum and energy equations are employed for the liquid and the vapor phase [8,9]. This method is widely used in nuclear engineering.

Several previous authors have reported preconditioning algorithms for multiphase mixtures. Kunz et al.[6] developed a code for the presence of a non-condensable gas. The governing equations, in which a separate continuity equation is used for an individual phase while the momentum equations are described for the mixture phase, were solved by using the preconditioning and the dual time stepping method. However, in this model, the compressibility effects were not account in the multiphase mixture region. Ahuja et al.[1] proposed multiphase preconditioning algorithms including the compressible effects. However, in these models the effects of temperature was neglected. More recently, Lindau et al.[8] and Owis et al.[10] have been presented the fully compressible multiphase flow models which have taken into account the

changes of both compressibility and temperature. The promising results were obtained with these two algorithms. A comparison of the performance of three different cavitation models, namely by Merkle et al.[9], Kunz et al.[11] and Singhal et al.[12], was given by Senocak and Shyy[13]. The comparison of surface pressure distribution over a hemispherical object gave a good agreement among these three models. However, the obtained density profiles do not reach an agreement, indicating that the cavitation models generate different compressibility characteristics.

The objective of the present work is to develop a base code for simulating cavitating flow past supercavitating torpedo including compressibility effects and interactions with hot plume of propulsive exhaust gas.

2. GOVERNING EQUATIONS AND NUMERICAL METHOD

Based on the homogeneous mixture model, the governing equation is comprised of the continuity equation for liquid and vapor phase and momentum equation in mixture phase as follows (Kunz et al.[6]):

$$\begin{aligned} \left(\frac{1}{\rho_m \beta^2} \right) \frac{\partial p}{\partial \tau} + \frac{\partial u_j}{\partial x_j} &= (\dot{m}^+ + \dot{m}^-) \left(\frac{1}{\rho_l} - \frac{1}{\rho_v} \right) \\ \frac{\partial \alpha_l}{\partial t} + \left(\frac{\alpha_l}{\rho_m \beta^2} \right) \frac{\partial p}{\partial \tau} + \frac{\partial \alpha_l}{\partial \tau} + \frac{\partial}{\partial x_j} (\alpha_l u_j) &= (\dot{m}^+ + \dot{m}^-) \left(\frac{1}{\rho_l} \right) \quad (1) \\ \frac{\partial}{\partial t} (\rho_m u_i) + \frac{\partial}{\partial \tau} (\rho_m u_i) + \frac{\partial}{\partial x_j} (\rho_m u_i u_j) &= - \frac{\partial p}{\partial x_j} + \frac{\partial}{\partial x_j} \left[\mu_{m,l} \left(\frac{\partial u_i}{\partial x_j} + \frac{\partial u_j}{\partial x_i} \right) \right] \end{aligned}$$

where the subscript l and v mean the liquid and vapor phase, respectively. The subscript m denotes the mixture phase. α is the volume fraction. τ is the pseudo-time for dual time stepping while t is the physical time. \dot{m}^+ and \dot{m}^- denote transformation of vapor to liquid and that of liquid to vapor, respectively, and will be mathematically modeled later. The density of the mixture phases is defined as:

$$\rho_m = \alpha_l \rho_l + \alpha_v \rho_v \quad (2)$$



$$\alpha_l + \alpha_v = 1 \quad (3)$$

The molecular viscosity, μ_m , is computed as

$$\mu_m = \alpha_l \mu_l + \alpha_v \mu_v \quad (4)$$

Turbulent eddy viscosity, μ_t , is obtained from Chien k- ϵ model [3] by using

$$\mu_t = \frac{\rho_m c_\mu f_\mu k^2}{\epsilon} \quad (5)$$

Rewriting Eq. (1) in generalized curvilinear coordinates,

$$\Gamma_e \frac{\partial \hat{q}}{\partial t} + \Gamma \frac{\partial \hat{q}}{\partial \tau} + \frac{\partial(\hat{E} - \hat{E}_v)}{\partial \xi} + \frac{\partial(\hat{F} - \hat{F}_v)}{\partial \eta} + \frac{\partial(\hat{G} - \hat{G}_v)}{\partial \zeta} = \hat{S} \quad (6)$$

where $\hat{q} = J[p \ u \ v \ w \ \alpha_l]^T$. \hat{E} , \hat{F} , and \hat{G} are the convective flux terms. \hat{E}_v , \hat{F}_v , and \hat{G}_v are viscous flux terms. The matrix, Γ_e and S are represented as:

$$\Gamma_e = \begin{pmatrix} 0 & 0 & 0 & 0 & 0 \\ 0 & \rho_m & 0 & 0 & u\Delta\rho_1 \\ 0 & 0 & \rho_m & 0 & v\Delta\rho_1 \\ 0 & 0 & 0 & \rho_m & w\Delta\rho_1 \\ 0 & 0 & 0 & 0 & 1 \end{pmatrix} \quad (7)$$

$$\hat{S} = J \left\{ (\dot{m}^+ + \dot{m}^-) \left(\frac{1}{\rho_l} - \frac{1}{\rho_v} \right), 0, 0, 0, (\dot{m}^+ + \dot{m}^-) \frac{1}{\rho_l} \right\}^T \quad (8)$$

where $\Delta\rho_i \equiv \rho_l - \rho_v$. The pre-conditioning matrix, Γ , is obtained from the modification of Γ_e to efficiently handle the stiffness problem.

$$\Gamma = \begin{pmatrix} \left(\frac{1}{\rho_m \beta^2} \right) & 0 & 0 & 0 & 0 \\ 0 & \rho_m & 0 & 0 & u\Delta\rho_1 \\ 0 & 0 & \rho_m & 0 & v\Delta\rho_1 \\ 0 & 0 & 0 & \rho_m & w\Delta\rho_1 \\ \left(\frac{\alpha_l}{\rho_m \beta^2} \right) & 0 & 0 & 0 & 1 \end{pmatrix} \quad (9)$$

where β is the preconditioning parameter (usually, set to $\beta^2 / U_\infty^2 \approx 10$). Cavitation model, based on Merkle et al.'s model [9], was used in this study. In this model, the mass transfer rate from liquid to vapor in a region where the local pressure is less than the vapor pressure is simply modeled as being proportional to the liquid volume fraction and the difference between the local and vapor pressures, as follows:

$$\dot{m}^- = \frac{C_{dest} \rho_v \alpha_l \min[0, p - p_v]}{(\rho_l U_\infty^2 / 2) t_\infty} \quad (10)$$

The mass transfer from vapor back to liquid in a region where

the local pressure exceeds the vapor pressure is given as follows:

$$\dot{m}^+ = \frac{C_{prod} \rho_v \alpha_l^2 (1 - \alpha_l)}{t_\infty} \quad (11)$$

The preconditioning system (1) is approximated with Euler implicit differencing for the artificial time term and second-order accurate backward differencing for the physical time. The viscous and inviscid flux terms are approximated by second-order central differences and by using the flux splitting procedure, respectively. The approximate system is then rewritten so that it can be solved as a series of sweeps in each coordinate direction with the use of the Block-Thomas scheme (Chapra and Canale, [2]). The second order implicit and forth order explicit artificial damping was added to the finite difference equation.

3. RESULTS AND DISCUSSION

Three different configurations of cylinder-hemispherical, 1-, and 0-caliber forebody-were used to validate the present code. Figure 1 shows surface pressure distribution on hemispherical forebody cylinder at several cavitation numbers, which compared with experiment[14]. Good agreements were attained over all tested cavitation numbers. At the downstream of the cavity the obtained results become a little underestimated. This discrepancy at these down stream sections may be related to an overestimation of the turbulent viscosity, which is due to the limitation of the k- ϵ turbulence model. Also, the fluid compressibility effects have not taken into account in the present model, which results the fact that the model cannot completely reflect physical phenomenon in high-compressible mixture case (say cavitation number $\sigma < 0.32$). Further discussion on the limitation of standard k- ϵ models can be referred in Ref. [3] and [4]. Figure 2 shows liquid volume fraction and surface pressure contours at $\sigma=0.3$, compared with numerical result by Kunz et al.[11]. In this figure, the present result shows well agreement with Kunz et al.'s result. Figure 3 shows velocity vectors, showing the velocity profiles of re-entrant jet. Figure 4 shows cavitating patterns at different cavitation numbers. Figure 5 shows the surface pressure distribution on the 1-caliber forebody cylinder at cavitation number of $\sigma=0.46, 0.40, 0.32$, and 0.24 . This figure has experimental data[14] to validate the present code. Figure 6 shows the liquid volume fraction and surface pressure contours of 1-caliber cylinder at $\sigma=0.24$. Figure 7 and 8 are corresponding to those of 0-caliber cylinder. Figure 9 shows 3-d viewgraph of cavitation pattern. Figure 10 shows time hysterical behavior of liquid volume fraction and streamlines at $\sigma=0.3$. Figure 11 is those by Venkateswam et al.[15]. Here, qualitatively good agreements were obtained. Figure 12 and 13 show the results of ALE-15 hydrofoil at $\sigma = 2.3$, $Re=2.12 \times 10^6$, and $\alpha = 5^\circ$. The velocity profiles and surface pressure on the hydrofoil was measured by Dular et al.[16]. Figure 14 shows well agreement of surface pressure on NACA 16012 hydrofoil with the result of Kunz et al.[17]. Figure 15 shows time evolution of cavitation and Figure 16 shows liquid volume fraction over the hemispherical forebody cylinder at $\sigma=0.3$ when the strong side flow of 15% of freestream speed was abruptly imposed. Figure 18 shows the comparison of vapor volume fraction with and without ventilation. The ventilation was circumferentially applied at the beginning location of shoulder with double strength of pressure and velocity relative to the freestream values.

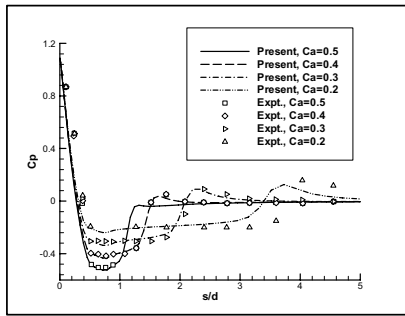
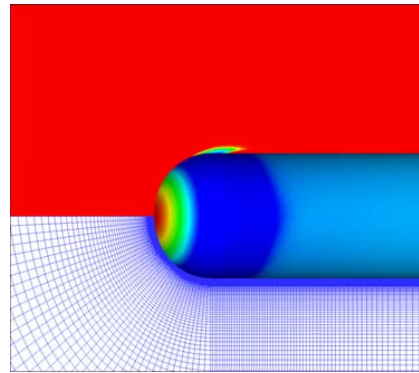
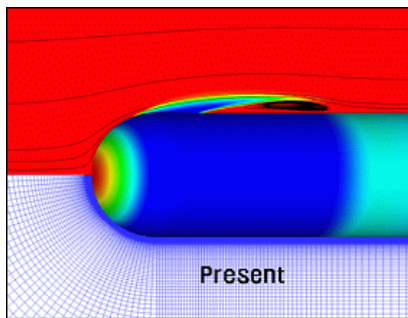


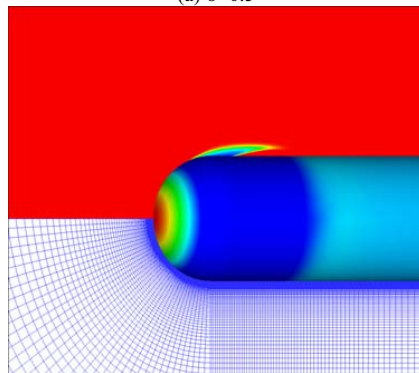
Fig. 1 Comparison of surface pressures at various cavitation numbers on hemispherical forebody



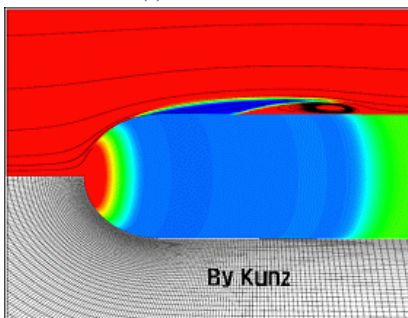
(a) $\sigma=0.5$



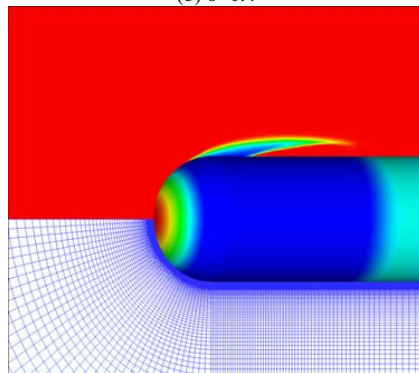
(a) Present result



(b) $\sigma=0.4$



(b) By Kunz et al.[11]



(c) $\sigma=0.3$

Fig. 2 Comparison of liquid volume fraction and surface pressure contours at $\sigma=0.3$

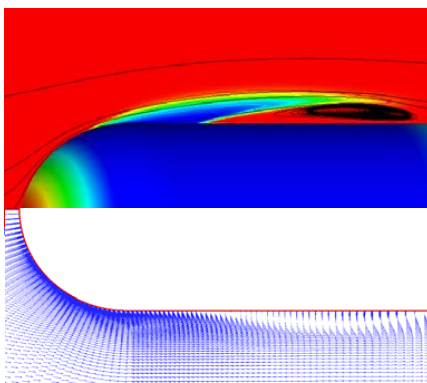
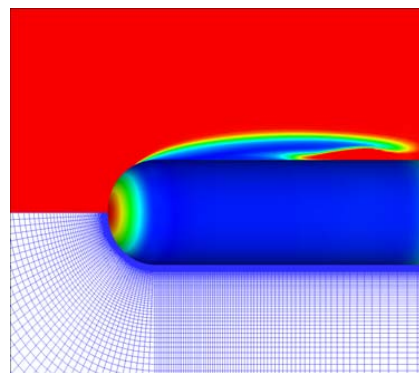


Fig. 3 Velocity vectors, streamlines, and liquid volume fraction of hemispherical forebody at $\sigma=0.3$



(d) $\sigma=0.2$

Fig. 4 Cavitating flow pattern at various cavitation number

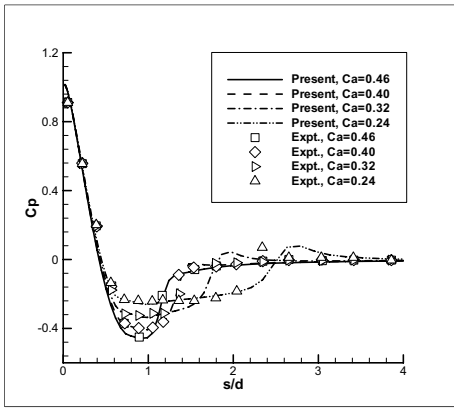


Fig. 5 Comparison of surface pressures at various cavitation numbers on 1-caliber forebody

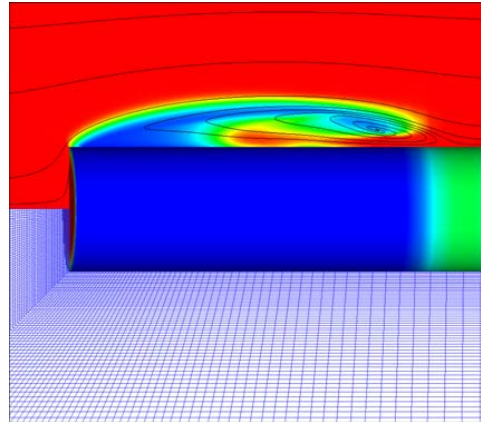


Fig. 8 Liquid volume fraction & surface pressure contours of 0-caliber cylinder at $\sigma=0.3$

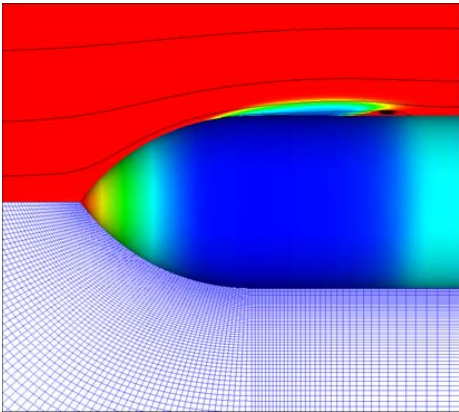
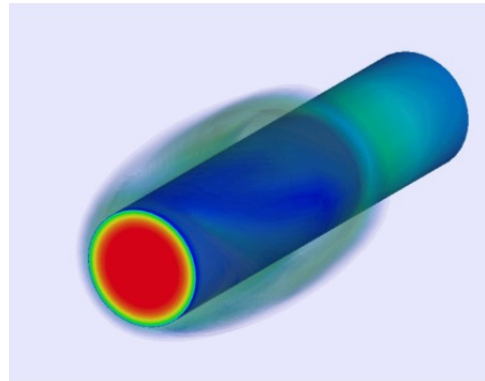


Fig. 6 Liquid volume fraction and surface pressure contours of 1-caliber cylinder at $\sigma=0.24$



(a) Present result

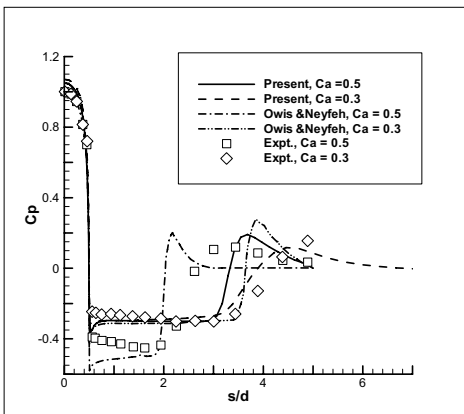
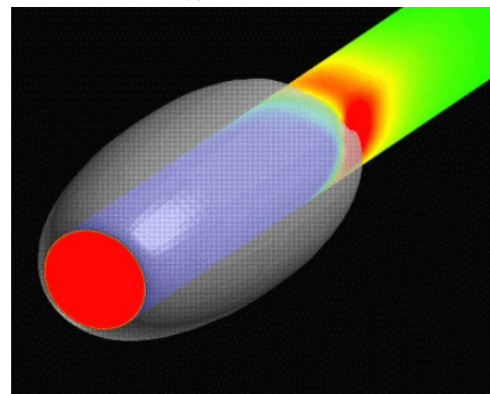


Fig. 7 Comparison of surface pressures at various cavitation numbers on 0-caliber cylinder



(b) Result by Kunz et al. [19]

Fig. 9 Comparison with liquid volume fraction of 0-caliber cylinder

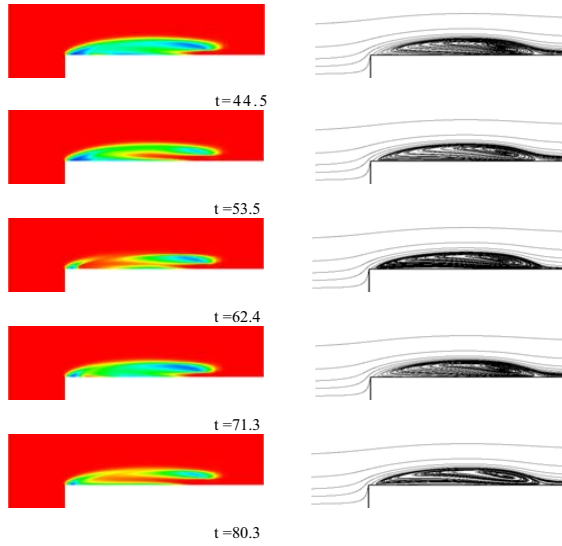


Fig. 10 Time sequence of liquid volume fraction and streamlines of 0-caliber cylinder

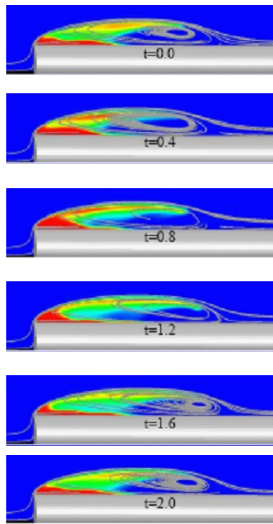
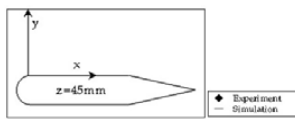
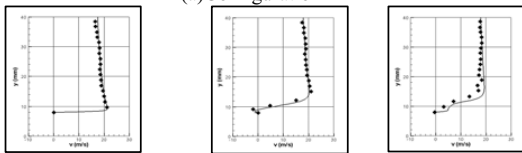


Fig. 11 Liquid volume fraction and streamline by Venkateswam et al.[15]



(a) Configuration

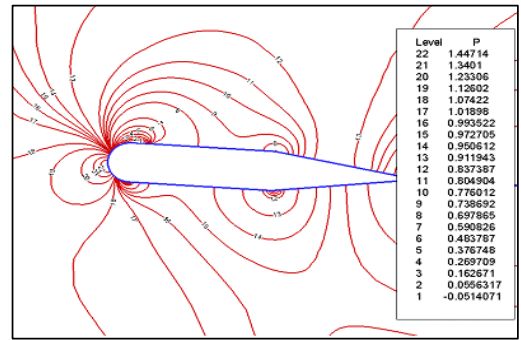


(b) 0mm

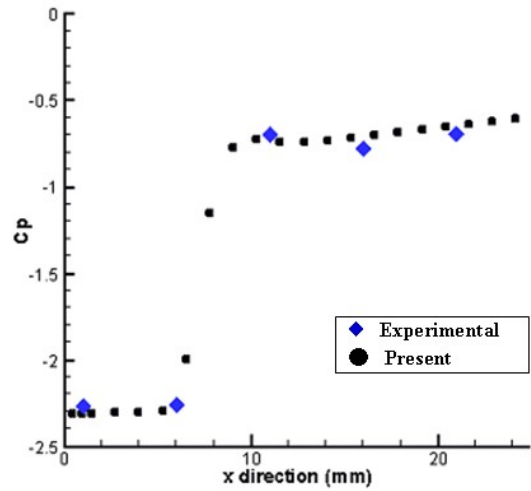
(c) 13mm

(d) 26mm

Fig. 12 Velocity profile of ALE-15 hydrofoil at $\sigma = 2.3$, $Re=2.12 \times 10^6$, and $\alpha = 5^\circ$



(a) Pressure Contour at $z = 15\text{mm}$



(b) Surface pressure coefficient at $z = 15\text{mm}$

Fig. 13 Comparison of pressure coefficient with other numerical result at $z = 15\text{mm}$ of ALE-15

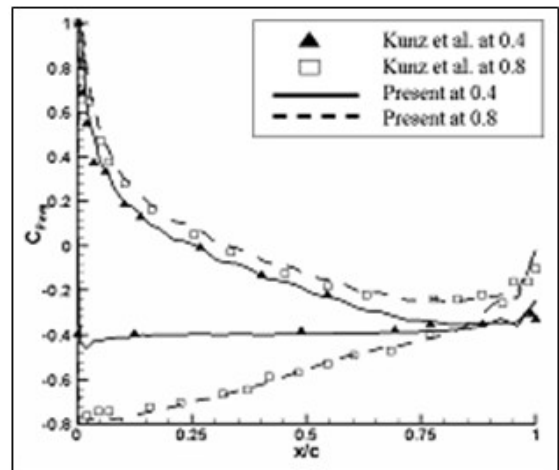


Fig. 14 Surface pressure of NACA 16012 hydrofoil at $\sigma = 0.4$ and 0.8 , $Re=2 \times 10^6$, and $\alpha = 7^\circ$, compared with Kunz et al.[17]

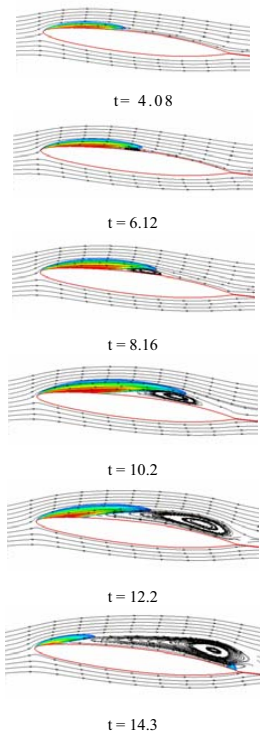


Fig. 15 Time sequence of liquid volume fraction of NACA 16012 hydrofoil

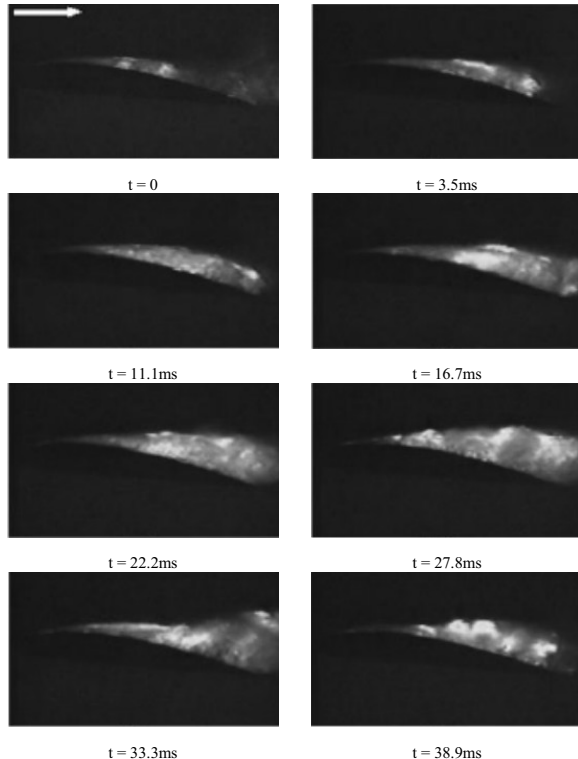


Fig. 16 Flow visualization experiment(Kawanami et al. [18])for Clark-Y hydrofoil

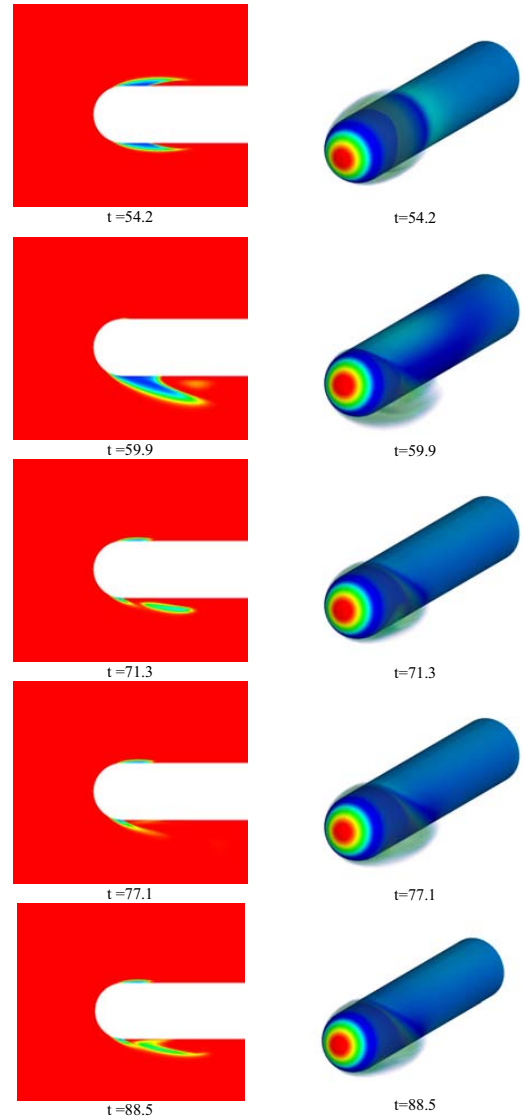


Fig. 17 Time sequence of liquid volume at $\sigma=0.3$ affected by strong side flow

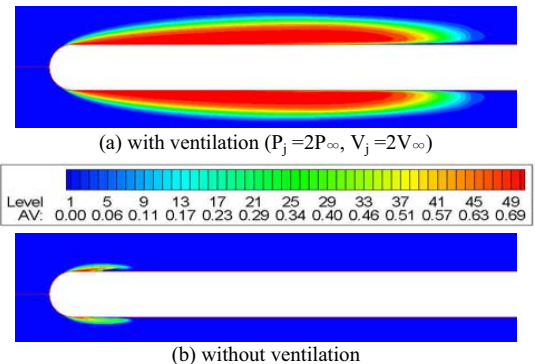


Fig. 18 Vapor volume fraction of hemispherical forebody with and without ventilation



4. CONCLUSION

The base solver for simulating the cavitating flows has been successfully developed. For code validation, the code has been applied cylinder with hemispherical, 1- and 0-caliber forebody and hydrofoil of ALE-15 and NACA 16012 cross-section. The present results have given fairly good agreement with experiments and other numerical results. The code also has shown the feasibility of the use for ventilated cavitation. The present base code will be improved to have the compressibility effects and interactions with hot plume of propulsive exhaust gas for supercavitating torpedo.

ACKNOWLEDGMENTS

This study was done by the support of Underwater Vehicle Research Center(UVRC), Agency for Defense Development(ADD), and Defense Acquisition Program Administration(DAPA) of Korea.

REFERENCES

- [1] 2001, Ahuja, V., Hosangadi, A., Arunajatesan, S., "Simulation of Cavitating Flow Using Hybrid Unstructured Meshes," *Journal of Fluids Engineering*, Vol.123, pp.331-340.
- [2] 1990, Kays, W.M and Crawford, M.E., *Heat transfer*, Wiley, New York, pp.256-258.
- [2] 2006, Chapra, S.C., and Canale, R.P., "Numerical Methods for Engineers," *Fifth Edition, McGraw-Hill Book Company*, New York.
- [3] 1982, Chien K.Y., "Prediction of Change and Boundary Layer Flows with a Low-Reynolds-Number Turbulence Model," *AIAA Journal*, Vol.22, pp.33-38.
- [4] 2003, Coutier-Delgosha O., Reboud, J.L. and Delannoy, Y., "Numerical Simulation of the Unsteady Behaviour of Cavitating Flows," *Int. J. Numer. Meth. Fluids Conference*, Vol.43, pp.527-548.
- [5] 2003, Coutier-Delgosha O., Patella, R. F. and Reboud, J. L., "Evaluation of the Turbulence Model on the Numerical Simulations of Unsteady Cavitation," *Journal of Fluids Engineering*, Vol.125, pp.38-45
- [6] 2000, Kunz, R.F., Boger, D.A., Stinebring, D.R., Chyczewski, T.S., Lindau, J.W., Gibeling H.J., Venkateswaran, S and Govindan, T.R., "A preconditioned Navier-Stokes method for two-phase flows with application to cavitation prediction," *Computers and Fluids*, Vol.29, pp.849-875.
- [7] 2003, Kunz, R.F., Lindau, J.W., Kaday, T.A. and Peltier, L.J., "Unsteady RANS and detached eddy simulations of cavitating flow over a hydrofoil," *CAV2003 5th International Symposium on Cavitation*, Paper No. CAV03-OS-1-12, Osaka, Japan.
- [8] 2003, Lindau, J.W., Venkateswaran, S, Kunz, R.F., Merkle, C.L., "Computation of Compressible Multiphase Flows," *AIAA 2003-1285*, 41st Aerospace Sciences Meeting and Exhibit, Reno, NV, USA.
- [9] 1998, Merkle, C.L., Feng, J.Z. and Buelow, P.E.O., "Computational Modeling of the Dynamics of Sheet Cavitation," *Proceedings of the 3rd International Symposium on Cavitation*, Grenoble, France.
- [10] 2003, Owis F.M. and Nayfeh A.H., "Computational of Compressible Multiphase Flow Over the Cavitating High-Speed Torpedo," *Journal of Fluids Engineering*, Vol.125, pp.459-468.
- [11] 1999, Kunz, R.F., Boger D.A., Chyczewski T.S., Stinebring D.R., Gibeling H. J. and Govindan T. R., "Multi-phase CFD analysis of natural and ventilated cavitation about submerged bodies.," *Proceedings of 3rd ASME/JSME Joint Fluids Engineering Conference*, ASME Paper FEDSM99-7364.
- [12] 2002, Singhal, A.K., Athavale, M.M., Li, H. and Jiang, Y., "Mathematical Basis and Validation of the Full Cavitation Model," *Journal of Fluids Engineering*, Vol.124, pp.617-624.
- [13] 2004, Senocak I and Shyy W., "Interfacial dynamics-based modeling of turbulent cavitating flows, Part-2: Time-dependent computations," *International Journal for Numerical Methods in Fluids*, Vol.44, pp.997-1016.
- [14] 1948, Rouse H. and McNown J.S., "Cavitation and Pressure Distribution," *Head Forms at Zero Angle of Yaw*, Stud. Engrg., Vol.32, State University of Iowa.
- [15] 2001, Venkateswaran, S., Lindau, J.W., Kunz, R.F. and Merkle, C.L., "Preconditioning Algorithms for Computation of Multi-Phase Mixture Flows," *AIAA 39th Aerospace Sciences Meeting & Exhibit*, AIAA Paper 2001-0125.
- [16] 2005, Dular, M., Bachert, R., Stoffel, B. and Širok, B., "Experimental evaluation of numerical simulation of cavitating flow around hydrofoil," *European Journal of Mechanics B/Fluids*, Vol.24, pp.522-538.
- [17] 2003, Kunz, R.F., Lindau, J.W., Kaday, T. A and Peltier, L. J, "Unsteady Rans Detached Eddy Simulations of Cavitating Flow of a Hydrofoil," *5th International Symposium on Cavitation(CAV2003)*, Osaka, Japan, CAV03-OS-1-12.
- [18] 1997, Kawanami Y, Kato H, Yamaguchi H, Tanimura M and Tagaya T., "Mechanism and control of cloud cavitation," *Journal of Fluids Engineering*, Vol.119, pp 788-94.
- [19] 2001, Lindau, J.W. and Kunz, R.F., Venkateswaran, S, Boger, D. A., "Application of Preconditioned, Multiple-Species, Navier-Stokes Models to Cavitating Flows," *Proceedings of the 4th International Symposium on Cavitation(CAV2001)*, Pasadena, USA. CAV01 session B4-005.